PAPER • OPEN ACCESS

The nuclei ^{12}C, ^{16}O and the role of the Pauli Exclusion Principle

To cite this article: P. O. Hess *et al* 2019 *J. Phys.: Conf. Ser.* **1308** 012011

View the article online for updates and enhancements.

The nuclei ^{12}C, ^{16}O and the role of the Pauli Exclusion Principle

P. O. Hess[1,2]**, M. Berriel-Aguayo**[1] **and L. J. Chávez-Nuñez**[1]

[1]Instituto de Ciencias Nucleares, UNAM, Circuito Exterior, C.U.,
A.P. 70-543, 04510 México D.F., Mexico
and
[2]Frankfurt Institute for Advanced Studies FIAS and Institute for Theoretical
Physics, J.W. Goethe - University Frankfurt, Germany

E-mail: [1]`hess@nculeares.unam.mx`

Abstract. We investigate the role of the Pauli Exclusion Principle (PEP) for light nuclei, at the examples of ^{12}C and ^{16}O. We show that ignoring the PEP does lead not only to a too dense spectrum at low energy but also to a wrong grouping into bands. Using a geometrical mapping, a triangular structure for ^{12}C and a tetrahedral structure in ^{16}O in the ground state is obtained by using the indistinguishably of the α-particles.

1. Introduction

The nuclei ^{12}C and ^{16}O play an important role in the investigation of α-cluster systems THSR,freer2017,funaki2010,schuck2013,schuck2017,funaki2018,review-clusters,schuck2018. No core shell model calculations have been performed [9, 10, 11] in order to understand, under several aspects, the structure of the Hoyle state. Also calculations within the *Antisymmetrized Molecular Dynamics* model (AMD)l [12, 13, 6] and within the *Orthogonality Condition Model* (OCM) [35] have been performed, using a microscopic Hamiltonian. These microscopic models lead to an understanding of the Hoyle state [15], important in the ^{12}C production in stars.

In [16, 17, 18] the *Algebraic Cluster model* (ACM) [19] has been applied to ^{12}C and ^{16}O, assuming in the first one a triangular structure and in the second one a tetrahedral structure. The ACM is purely algebraic and does not take into account the *Pauli Exclusion Principle* (PEP). The bands are obtained by rotating the classical geometrical structure and bands are differentiated according to their vibrational structure.

In [20] the ^{12}C nucleus was investigated within the *Semimicroscopic Algebraic Cluster Model* (SACM) [21, 22], which is also an algebraic model, but whose model space takes into account the PEP. The similarity to the ACM makes this model ideal to compare to the ACM. The main conclusions in [20] are: i) The association of bands

Role of the Pauli principle

in the ACM is not consistent, the projection to Pauli allowed states leads to a grouping of bands according to the $SU(3)$ shell model *irreducible representations* (irrep). ii) Not including the PEP leads to too many states at low energy. Doublets predicted in the ACM are not there any more. iii) The additional (second) 5^- state at low energy is not supported by the shell model. iv) the observation of the 5^- state in [16] does not prove a triangular structure, it is just part of a band which is obtained in all models. v) Applying a geometrical mapping, for the ground state band it is trivial that ^{12}C has a triangular and ^{16}O a tetrahedral structure. The reason is that the α-particles are indistinguishable and, thus, the distance between any two α particles must be the same. For higher bands different geometrical configurations may mix and the situation is not very clear.

   In this contribution we will report in more detail on these findings and include some new results on ^{16}O. The complete results will be published elsewhere.

   In Section 2 the SACM is briefly resumed and the Hamiltonian used for ^{12}C is presented. Results and the discussion will also be provided. Finally, in Section 3 conclusions will be drawn.

2. The model, Hamiltonian and Quadrupole operator

Within the SACM [21, 22] the clusters are treated within the shell model and are in their ground state. The whole nucleus is also treated within the shell model and is a sum of the two clusters with the addition of the relative motions between the clusters. Each relative motion is quantized by the relative oscillation creation and annihilation operators $\boldsymbol{\pi}^\dagger_{\lambda_k,m}$ and $\boldsymbol{\pi}_{\lambda_k,m}$, respectively, where λ_k refers to the k'th Jacobi coordinate. The generators of the relative motion in the k'th Jacobi coordinate are given by $\boldsymbol{C}^{m'}_m(k) = \boldsymbol{\pi}^\dagger_m(k)\boldsymbol{\pi}^{m'}(k)$ and the ones related to the sum over all relative vibrations are $\boldsymbol{C}^{m'}_m = \sum_k \boldsymbol{\pi}^\dagger_m(k)\boldsymbol{\pi}^{m'}(k) = \boldsymbol{\pi}^\dagger_m\boldsymbol{\pi}^{m'}$. Auxiliary scalar bosons $\boldsymbol{\sigma}^\dagger$ and $\boldsymbol{\sigma}$ are introduced in order to implement a cutoff value N, with $N = n_\pi + n_\sigma$, where n_π and n_σ are the number operators of the total number of π oscillations and of the number of σ-bosons. The σ-bosons have no physical meaning, save for the cut-off. The number of relative motion quanta in each Jacobi coordinate is limited from below by the *Wildermuth condition* [23], which is a minimal condition for satisfying the PEP. Multiplying the $SU(3)$ irreps of the clusters with the relative motion leads to a sum of total $SU(3)$ irreps which still in part do not satisfy the PEP. These are excluded by constructing the overlap of the list of irreps obtained by the list of the shell model $SU(3)$ irreps. This is a quite brief summary and for more details, please consult the original publications on the SACM [21, 22].

   The model Hamiltonian proposed for ^{12}C is

Role of the Pauli principle

$$\begin{aligned}
\boldsymbol{H} = {}& \hbar\omega\boldsymbol{n}_\pi - \chi\boldsymbol{\mathcal{C}}_2(\lambda,\mu) + t_2(\boldsymbol{\mathcal{C}}_2(\lambda,\mu))^2 + t\boldsymbol{\mathcal{C}}_3(\lambda,\mu) \\
& + \left(a + a_L(-1)^L + a_{Lnp}\Delta\boldsymbol{n}_\pi\right)\boldsymbol{L}^2 + b\boldsymbol{K}^2 \\
& + b_1\left[\left(\boldsymbol{\sigma}^\dagger\right)^2 - \left(\boldsymbol{\pi}^\dagger\cdot\boldsymbol{\pi}^\dagger\right)\right]\cdot[h.c.] \quad .
\end{aligned} \tag{1}$$

The first term is just the harmonic oscillator field and the $\hbar\omega$ is fixed via $45\times A^{-1/3}-25\times A^{-2/3}$ [24], where its value is 14.89 for ^{12}C. The second term is related to the algebraic quadrupole-quadrupole interaction [25], with $\boldsymbol{\mathcal{C}}_2(\lambda,\mu)$ being the second order Casimir operator. The third and fourth terms allow for corrections in the relative ordering of $SU(3)$ irreps, where $\boldsymbol{\mathcal{C}}_3$ is the third order Casimir operator, which distinguishes between (λ,μ) and (μ,λ). The fifth term allows to describe changes in the moment of inertia for states with higher shell excitations and when the spin parity changes. The last term in the second line lifts the degeneracy in angular momentum for states within the same $SU(3)$ irrep. Up to here, the Hamiltonian is within the $SU(3)$ limit and permits analytic results, substituting the operators by their corresponding eigenvalues. In the last line, the term mixes $SU(3)$ irreps, it is a generator of a $O(4)$ group. The pure $SU(3)$ part has 7 free parameters, the same as in [16] (including N). For allowing the mixing a further parameter (b_1) is added, i.e., in the final calculations there are 8 parameters.

As the quadrupole transition operator we use the one given in [26], which is a symplectic generator, including connections to multiple $2\hbar\omega$ shell excitations. In an algebraic model it is customary to use the algebraic part of this operator, which does not connect shells, valid when inter-shell excitations are not considered. The physical quadrupole operator [26, 27] is given by

$$\begin{aligned}
\boldsymbol{Q}_{2m}^{phys} &= Q_{2m}^a + \frac{\sqrt{6}}{2}\left(\boldsymbol{B}_{2m}^\dagger + \boldsymbol{B}_{2m}\right) \\
\boldsymbol{B}_{2m}^\dagger &= \left(\boldsymbol{\pi}^\dagger\cdot\boldsymbol{\pi}^\dagger\right), \ \boldsymbol{B}_{2m} = \left(\boldsymbol{\pi}\cdot\boldsymbol{\pi}\right) \quad .
\end{aligned} \tag{2}$$

The $\boldsymbol{B}_{2m}^\dagger$ operator transforms as a (2,0) $SU(3)$ irrep, while $\boldsymbol{B}_{2m}$ as its conjugate.

The states for the 3-α cluster nucleus ^{12}C and the 4-α cluster nucleus ^{16}O were constructed, using the work done in [29, 30]. The overlap of the symmetrized cluster states with the shell model is determined using spin-isospin zero supermultiplets [31] to which the total state is coupled. The microscopic model space for ^{12}C is given in [20] and for ^{16}O it will be published elsewhere.

In Fig. 1 several fits, each referring to the adjustment to the $B(E2; 0_2^+ \to 2_1^+)$-value, are depicted. The general agreement is quite good and comparable to the one given in [16]. However, the ordering into bands is completely different. The $SU(3)$ fit indicates that the bands are ordered according to definite $SU(3)$ irreps. In each irrep, the states have a definite deformation, as deduced in [32, 33]. Thus, intrinsic states with different deformation are associated into different bands!
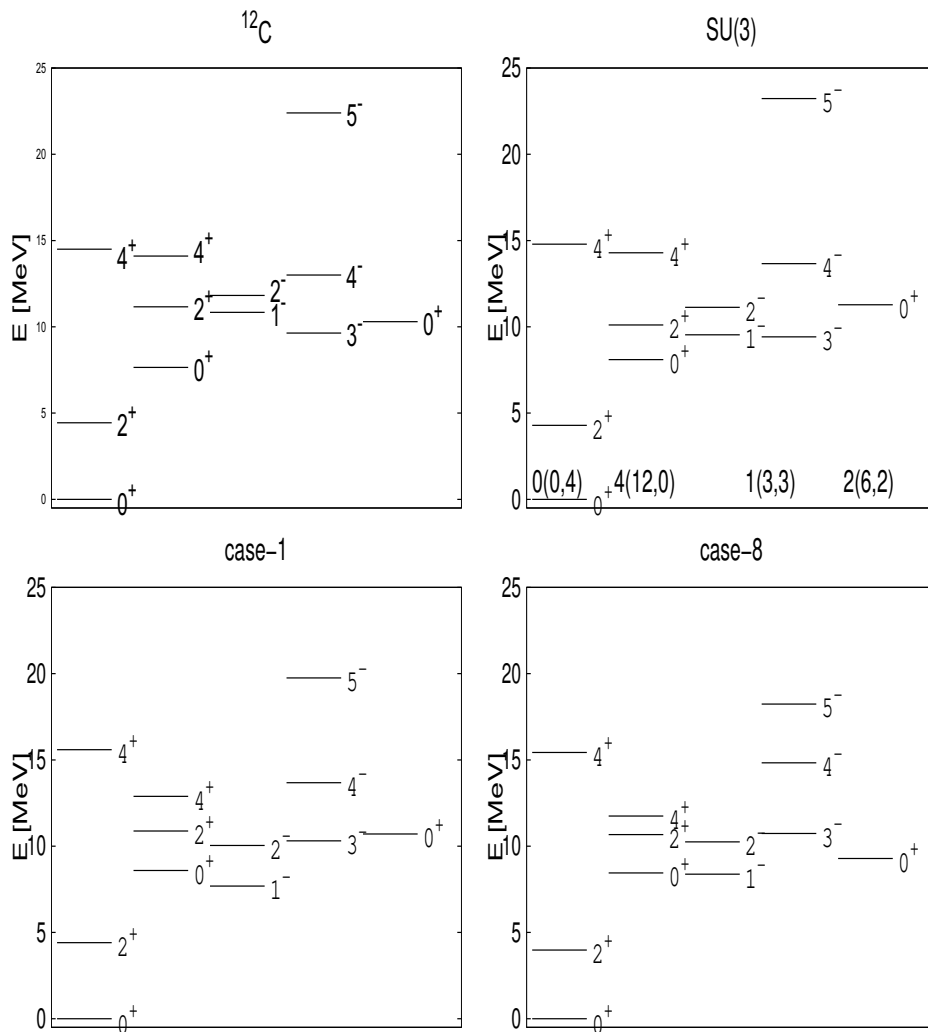
Role of the Pauli principle

Figure 1. Spectrum of ^{12}C. In the upper row, the left figure is the experimental spectrum and the right figure depicts the result for pure $SU(3)$. In the second row, the left figure depicts the result when the $B(E2; 0_2^+ \to 2_1^+)$ transition value is adjusted to 1 WU and the right figure when this value is adjusted to the experimental one, namely 8 WU, which is the value from experiment [28]. The first excited 0^+ state corresponds to the hoyle state [15]. The experimental values are taken from [28]. In the $SU(3)$ plot, at the lower part the numbers $\Delta n_\pi (\lambda, \mu)$ are listed, where Δn_π refers to the shell exciations and (λ, μ) to the corresponding $SU(3)$ irrep.

In Fig. 2 we compare the case where the $B(E2; 2_1^+ \to 0_1^+)$ is adjusted to 1 WU (left panel) to the results of the ACM [16]. As seen, the spin-doublets are dissolved and the density of states is lower.

In Table 1 the $SU(3)$-content of the first two 0^+ bands are listed, where the values were rounded off. The association of states into the same band requires that the content is the same, however, in reality mixing effect reproduce only approximate agreements. As can be seen, the 2_1^+ state has a very similar content as the 0_1^+ state, thus, they belong to the same band. It is similar for the second 0^+ band. This cannot be concluded from
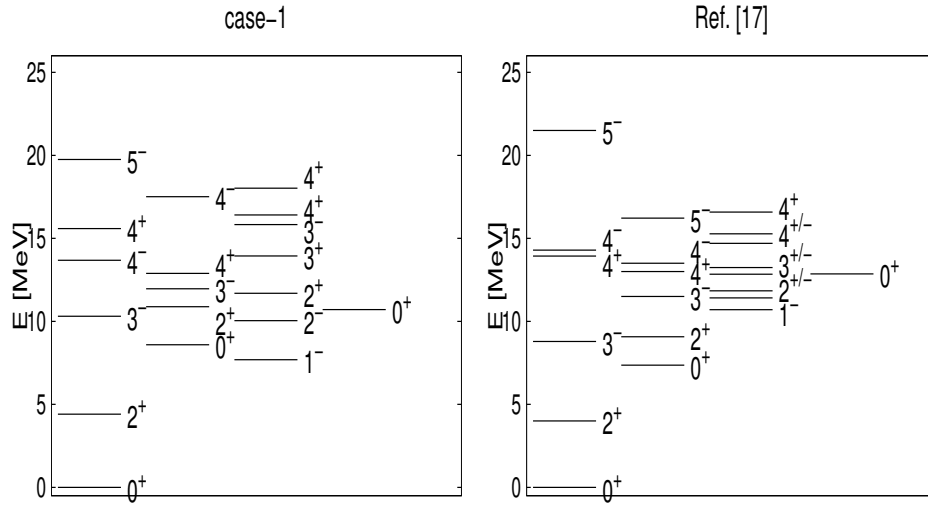
Role of the Pauli principle

Figure 2. Comparison Spectrum of ^{12}C, as calculated within the SACm (left panel) to the AMC (right panel).

L_i^π	0_1^+	2_1^+	4_2^+	0_2^+	2_2^+	4_1^+
$n_\pi = 4$:(0,4)	82	82	48	8	3	31
$n_\pi = 6$:(2,4)	16	16	4	22	41	16
$n_\pi = 6$:(4,3)	0	0	0	0	0	0
$n_\pi = 8$:(4,4)	1	2	0	22	28	29
$n_\pi = 8$:(6,2)	0	0	0	5	6	0
$n_\pi = 8$:(6,3)	0	0	0	0	0	0
$n_\pi = 8$:(8,2)	0	0	0	2	6	0
$n_\pi = 8$:(12,0)	0	0	0	33	6	0
$n_\pi = 10$:(6,4)	0	0	39	7	9	19
$n_\pi = 10$:(10,2)	0	0	0	0	0	0

Table 1. $SU(3)$ content of some low lying states with positive parity, given as in percent, for the case of $B(E2; 0_2^+ \rightarrow 2_1^+) = 8\, WU$. The numbers are only approximate and not all irreps are shown.

$B(EL; J_i^\pi \rightarrow J_f^\pi)$ [WU]	EXP.	$SU(3)$	case-1	case-8
$B(E2; 2_1^+ \rightarrow 0_1^+)$	4.65	4.65	5.18	3.41
$B(E2; 0_2^+ \rightarrow 2_1^+)$	8.	0.0	0.97	8.33
$B(E3; 3_1^- \rightarrow 0_1^+)$	12.	6.32	5.27	24.28

Table 2. List of $B(EL)$-transition values, measured and obtained in three different model calculations: In the first column information is listed on the type of the electromagnetic transition, the second column lists the corresponding experimental value, the third column assumes exact $SU(3)$ symmetry and in the last two columns the experimental value of $B(E2; 2_2^+ \rightarrow 0_1^+)$ is adjusted to different values (case-1: 1WU, case-8: 8WU).

Role of the Pauli principle

$B(EL; J_i^\pi \to J_f^\pi)$ [WU]	EXP.	case-1	Ref. [16]
$B(E2; 2_1^+ \to 0_1^+)$	4.65 ± 0.25	5.18	5.15
$B(E2; 0_2^+ \to 2_1^+)$	8.03 ± 1.10	0.97	0.80
$B(E3; 3_1^- \to 0_1^+)$	12.65 ± 1.99	12.23	5.15

Table 3. List of $B(EL)$-transition values, measured (first column), the one obtained within the SACM (second column) and within the ACM (third column). The numbers are given in WU.

the 4_1^+ and 4_2^+ states, which are already well mixed states, due to the large deformation of the ^{12}C nucleus. Here, the association into the bands is done in the eye of the beholder.

In Table 2 some experimental measured $B(E2)$ values and the $B(E3; 3_1^- \to 0_1^+)$ value are listed and compared to the $SU(3)$ calculation and two cases of theoretical fits, one where the side-band $B(E2; 0_2^+ \to 2_1^+)$ transition value is adjusted to 1 WU (as in [19]), called case-1, and another fit where this side-band transition value is adjusted to 8 WU, called case-8. The $B(E2)$-values were multiplied by a common scale factor $a \approx \frac{1}{2}$, which is proportional to the scale factor β^4 in [19]. The scale factor for the $B(E3)$ value is $a^{\frac{3}{2}}$, using the proportionality to β^6 [19]. The values for the $B(3)$ transition, listed in Table 2, were not multiplies by this factor. In the last column of Table 3 the corresponding $B(EL)$-values of the AMC, taken from [19], are listed and compared to the SACM and experimental values. In general, both theories are of the same quality. In the SACM the $B(E3; 3_1^- \to 0_1^+)$ is even better reproduced, it shows that the argument of a large $B(E3)$-value does not confirm the ACM. The main difference obviously shows up in the spectrum, suggesting that an effort has to be taken to measure if possible all states at low energy.

Why this difference to the ACM? In the ACM the α-particles are treated as independent classical objects and no antisymmetrization is performed. In ^{12}C they are located on the edges of a triangle and in ^{16}O on the edges of a tetrahedron. Upon this *classical* picture it is direct to create rotational bands, leading to the irreps of the corresponding discrete group. The problem with this is that the states are not antisymmetrized. By implementing the PEP these states are *projected* to Pauli allowed states, which destroys completely the ordering into irreps of the discrete groups. The final ordering is according to $SU(3)$ irreps in a pure $SU(3)$ model, and approximately when mixing is taken into account. The projection has nothing to do with a dynamical symmetry breaking within an algebraic model, because the states obtained in such a manner have still contributions which are not Pauli allowed.

An important feature, proven in [34, 35], is that the antisymmetrization between two clusters (PEP) produces an effective repulsive potential, i.e., that the fermions (nucleons) try to avoid to be at the same place This was later shown for two clusters in a different context [36], where after a geometrical mapping, the two clusters have a finite distance, a consequence that the Wildermuth condition [23], which requires a minimal number of oscillation quanta. Within the ACM, one can in principle simulate

Role of the Pauli principle

the repulsive potential, however, adding high order terms in the generators. Because this is not done, the Pauli exclusion effect is not taken into account.

This can also be illustrated within a geometrical mapping, where a trial state $| \alpha \rangle$ is defined, with the the recommendation to use a coherent state. The expectation value of the Hamiltonian with respect to this trial state defines a classical potential. The description works fine for the ground state band. Using a coherent state, which describes α-clusters [36, 20] in the ground state, the ^{12}C has to be a triangle and ^{16}O has to be a tetrahedron. This is due to the indistinguishably of the α-particles: The distance between any two of those has to be the same. While for the ground state band in ^{12}C a triangular structure and in ^{16}O a tetrahedral structure is obtained, for the excited bands this is not necessarily the case due to the mixing of several geometrical configurations. Also, in the case of ^{12}C the AMC model shows a triangular structure in the density profile in one calculation [2], while the density profile is much more compact in another AMC calculation [37] and the nucleus looks like an oblate deformed nucleus.

As mentioned above, the projection to Pauli allowed states destroys this classical picture, the nuclei in consideration not only have an overlap to an α-cluster state but consist principally of nucleons which are in an antisymmetric state.

The conclusions drawn for ^{12}C are the same for ^{16}O. The difference is that while ^{12}C has a strong deformation, ^{16}O is spherical and is a showcase for the $SU(3)$ shell model. All states can be described within the SACM as nearly pure $SU(3)$ states. The ACM still predicts too many states at low energy (many doublets) which are not supported by the shell model. Details will be published elsewhere.

3. Conclusions

The SACM, which satisfies the PEP, was compared to the ACM, which does not consider the PEP. It was shown that in both systems, ^{12}C and ^{16}O, the PEP is still important due to the large overlap of the α-particles. Projecting the ACM states to Pauli allowed states destroys the association into bands as done in the ACM. The ACM obtains too many states/doublets at low energy and some which are not there. The concepts of atomic molecular molecules cannot be applied to nuclear molecules directly, however, one has to supplement it by the PEP.

In conclusion, the PEP cannot be neglected!

The ACM can be improved when the Pauli exclusion principle is taken into account via a repulsive potential between the α-particles, as discussed in the text. However, this requires high order interaction terms, which the ACM in its present form does not consider.

Role of the Pauli principle

[1] A. Tohsaki, H. Horiuchi, P. Schuck and G. Röpke, Phys. Rev. Lett. **87** (2001), 192501.

[2] M. Freer, Rep. Prog. Phys. **70** (2007) 2149.

[3] Y. Funaki, M Girod, H Horiuchi, G Röpke, P Schuck, A Tohsaki and T Yamada, J. Phys. G: Nucl. Part. Phys. **37** (2010) 064012.

[4] P Schuck, J. Phys.: Conf. Ser. **436** (2013), 012065

[5] P. Schuck, Y. Funaki, H. Horiuchi, G. Röpke, A. Tohsaki and T. Yamada, Phys. Srcip.**91** (2016), 123001

[6] Y. Funaki, Phys. Rev. C **97** (2018), 021304(R).

[7] M. Freer, H. Horiuchi, Y Kanada-En'yo, D. Lee and U.-G. Meissner, Rev. Mod. Phys. **90** (2018), 035004.

[8] P. Schuck, AIP Conference Proceedings **2038** (2018), 020002

[9] A.C. Dreyfuss, K.D. Launey, T. Dytrych, J.P. Draayer, C. Bahri, Phys. Lett. B **727** (2013), 511.

[10] T. Dytrych, *Evidence for Symplectic Symmetry in ab initio no-core Shell Model Results*, (PhD Thesis, Lousiana State Universiuty, 2008).

[11] K. D. Launey, T. Dytrych and J. P. Draayer, Progr. in Part. and Nucl. Phys. **89** (2016), 101.

[12] Y. Kanada-En'yo, H. Horiuchi, and A. Ono, Phys. Rev. C 52, 628 (1995)

[13] Y. Kanada-En'yo and H. Horiuchi, ibid. 52, 647 (1995).

[14] S. Saito, Prog. Theor. Phys. 41 (1969), 705.

[15] F. Hoyle, Ap. J. Suppl. **1** (1954), 121.

[16] D. J. Marín-Lámbarri, R. Bijker, M. Freer, et al., Phys. Rev. Lett. **113** (2014), 012502.

[17] R. Bijker and F. Iachello, Phys. Rev, Lett. **112** (2014), 152501.

[18] R. Bijker and F. Iachello, Nucl. Phys. A **957** (2017), 154.

[19] R. Bijker and F. Iachello, Ann. Phys. (N.Y.) **298** (2002), 334.

[20] P. O. Hess, Eur. Phys. J. A **54** (2018), 32.

[21] J. Cseh, Phys. Lett. B **281** (1992), 173.

[22] J. Cseh and G. Lévai, Ann. Phys. (N.Y.) **230** (1994), 165.

[23] K. Wildermuth and Y. C. Tang, *A Unified Theory of the Nucleus*, (Academic Press, New York, 1977).

[24] J. Blomqvist and A. Molinari, Nucl. Phys. A **106** (1968), 545.

[25] J. P. Elliott, Proc. R. Soc. London A **245**, (1958) 128; **245** (1958), 562.

[26] O. Castaños and J. P. Draayer, Nucl. Phys. A **491** (1989), 349.

[27] O. Castaños, P. O. Hess, P. Rocheford and J. P. Draayer, Nucl. Phys. A **524** (1991), 469.

[28] www.nndc.bnl.gov/ensdf

[29] M. Moshinsky and Y. Smirnoc. *The Harmonic Oscillator inModern Physics*, (Harwood Academic Publishers, Australia, 1996).

[30] V. C. Aguilera-Navarro, M. Moshinsky and P. Kramer, Ann. Phys. **54** (1969), 379.

[31] E. Wigner, in *Group Theoretical Concepts and Methods in Elementary Particle Physics*, ed. by. F. Gürsey., (Gordon and Breach, New York, 1964).

[32] D J Rowe, Rep. Prog. Phys. **48** (1985), 1419.

[33] O. Castaños, J. P. Draayer and Y. Leschber, Z. f. Phys. A**329** (1988), 33.

[34] S. Saito, Prog. Theor. Phys. **40** (1968), 893.

[35] S. Saito, Prog. Theor. Phys. **41** (1969), 705.

[36] P. O. Hess, G. Lévai and J. Cseh, Phys. Rev. C **54** (1996), 2345.

[37] Y. Kanada-En'yo, Phys. Rev. C **96** (2017), 034306.